Front. Optoelectron. 2020, 13(3): 265–271
https://doi.org/10.1007/s12200-020-1041-z

RESEARCH ARTICLE

Polymer hole-transport material improving thermal stability of inorganic perovskite solar cells

Shaiqiang MU[1,2], Qiufeng YE[2,3], Xingwang ZHANG[2,3], Shihua HUANG (✉)[1], Jingbi YOU (✉)[2,3]

1 Physics Department, Zhejiang Normal University, Jinhua 321004, China
2 Key Laboratory of Semiconductor Materials Science, Institute of Semiconductors, Chinese Academy of Sciences, Beijing 100083, China
3 Center of Materials Science and Optoelectronics Engineering, University of Chinese Academy of Sciences, Beijing 100049, China

Abstract Cesium-based inorganic perovskite solar cells (PSCs) are paid more attention because of their potential thermal stability. However, prevalent salt-doped 2,2′,7,7′-tetrakis(N,N-dipmethoxyphenylamine)9,9′-spirobifluorene (Spiro-OMeTAD) as hole-transport materials (HTMs) for a high-efficiency inorganic device has an unfortunate defective thermal stability. In this study, we apply poly (3-hexylthiophene-2,5-diyl) (P3HT) as the HTM and design all-inorganic PSCs with an indium tin oxide (ITO)/SnO_2/LiF/$CsPbI_{3-x}Br_x$/P3HT/Au structure. As a result, the $CsPbI_{3-x}Br_x$ PSCs achieve an excellent performance of 15.84%. The P3HT HTM-based device exhibits good photo-stability, maintaining ~80% of their initial power conversion efficiency over 280 h under one Sun irradiation. In addition, they also show better thermal stability compared with the traditional HTM Spiro-OMeTAD.

Keywords inorganic perovskite solar cell (PSC), hole-transport material (HTM), stability

1 Introduction

In the past 10 years, the power conversion efficiency (PCE) of organic–inorganic hybrid perovskite solar cells (PSCs) has skyrocketed from 3.8% to 25.2% [1,2] because of their excellent optoelectronic properties, including high absorption coefficient [3,4], high carrier mobility [5], long balanced carrier diffusion length [6], and low exciton binding energy [7]. However, organic–inorganic hybrid PSCs face poor thermal stability caused by the organic compound [8]. The severe stability issue of PSCs could be effectively released when an inorganic cation, such as Cs^+, partially or fully substitutes the organic cations [9,10].

For the stability issue of the all-inorganic PSCs, apart from the intrinsic phase stability, the selection of hole-transport material (HTM) has also shown a significant effect [11]. The most commonly employed HTMs in inorganic PSCs are still 2,2′,7,7′-tetrakis(N,N-dipmethoxyphenylamine)9,9′-spirobifluorene (Spiro-OMeTAD) and poly[bis(4-phenyl) (2,4,6-trimethylphenyl)amine] (PTAA) [12–21]. You and colleagues simultaneously prepared a $CsPbI_3$ device with the indium tin oxide (ITO)/SnO_2/$CsPbI_3$/Spiro-OMeTAD/Au structure in a completely dry nitrogen environment and obtained 15.7% PCE [12]. Zhao et al. fabricated a perovskite device with the ITO/c-TiO_2/$CsPbI_3$/Spiro-OMeTAD/Ag structure and gained an excellent performance of 19.09% [13]. Meanwhile, Liu et al. applied PTAA as the HTM for the $CsPbI_3$ device and achieved 15.07% PCE [14]. In these hole-transport materials, the dopant bis(trifluoromethane) sulfonamide lithium salt and 4-tertbutylpyridine, which promote conductivity and proton transfer, are easily precipitated when the device suffers from heating [22–24]. Therefore, exploring a dopant-free hole-transport layer is critical for delivering efficient and stable inorganic perovskite solar cells.

Poly(3-hexylthiophene-2,5-diyl) (P3HT) is a very conventional polymer with a very high mobility (10^{-3} $cm^2/(V \cdot s)$). It has been successfully used in organic–inorganic hybrid solar cells [25]. In this work, we applied P3HT in all-inorganic PSCs with the ITO/SnO_2/LiF/$CsPbI_{3-x}Br_x$/P3HT/Au structure. As a result, the all-inorganic $CsPbI_{3-x}Br_x$ PSCs achieved an excellent performance of 15.84%. In addition, the P3HT HTM-based device exhibited good photo-stability, maintaining ~80% of its initial PCE over 280 h under one Sun irradiation. The device also showed better thermal stability compared to the traditional hole-transport material, Spiro-OMeTAD.

Received April 22, 2020; accepted May 9, 2020

E-mails: huangshihua@zjnu.cn, jyou@semi.ac.cn

2 Experiment

2.1 Materials

The SnO_2 nanoparticle precursor was purchased from Alfa Aesar (tin (IV) oxide, 15% in H_2O colloidal dispersion). Lead iodide (PbI_2), lead bromide ($PbBr_2$), N,N-dimethylformamide (DMF), dimethyl sulfoxide (DMSO), and chlorobenzene were obtained from Sigma-Aldrich. Spiro-OMeTAD was purchased from Xi'an Polymer Light Technology Corp. (China). Cesium iodide (CsI) was obtained from Aladdin Industrial, Corp. (China). P3HT was purchased from Solarmer (China).

2.2 Device fabrication

An ITO glass was cleaned by detergent, deionized (DI) water, acetone, and isopropanol in turn before drying in a N_2 flow. Next, the ITO substrate was cleaned by ultraviolet-ozone (UVO) treatment for 20 min, coated with the SnO_2 nanoparticle precursor at a speed of 3000 r/min for 30 s, and annealed at 150°C for 30 min in ambient air. Afterwards, the SnO_2/ITO substrate was disposed by UVO for 10 min. The perovskite film was prepared by the common one-step method. CsI (1 mol/L), $HPbI_3$ (0.68 mol/L), and $PbBr_2$ (0.32 mol/L) were then dissolved in a DMF–DMSO mixture (1:1.4 volume ratio) and stirred for 2 h. The PSC precursor was spun on the SnO_2 layer at 2600 r/min for 60 s, let stand by at room temperature for 1 h, and annealed at 170°C in ambient air for 10 min with humidity $< 40\%$. Subsequently, 30 μL P3HT solution with 10 mg/mL in chlorobenzene was spun on PSC 3000 r/min for 30 s and annealed at 100°C for 1 h. Finally, the electrode Au was coated by thermal evaporation with 80 nm thickness.

2.3 Device characterization

The photocurrent density–voltage (*J–V*) characteristic of the perovskite solar cell was finished by a Keithley 2400 ion source meter under one solar (AM 1.5 G) illumination using a solar simulator (EnliTech, Taiwan, China), and the KG-5 Si photodiode was used to calibrate the light intensity of the solar simulator. The photovoltaic cells were measured in a nitrogen glove box with reverse (1.2 V → 0 V, step 0.02 V) and forward (0 V → 1.2 V, step 0.02 V) scans. The scan electron microscopy image included the morphology and the cross-sectional structure of the device. Ultraviolet light was measured by a Varian Cary 5000 spectrophotometer. The photoluminescence (PL) spectrum was recorded using a FLS980 spectrometer (UK). The time-resolved PL spectra were measured by a F900 spectrometer (UK). The external quantum efficiency (EQE) curve was measured using the Taiwan EnliTech EQE measurement system (China). For the light stability test, unpackaged PSCs were immersed in a nitrogen glove box and in a continuous illumination using a white LED lamp (AM 1.5G, 100 mW/cm^2).

3 Results and discussion

We prepared the all-inorganic $CsPbI_{3-x}Br_x$ solar cell with the ITO/SnO_2/LiF/$CsPbI_{3-x}Br_x$/P3HT/Au structure as shown in Fig. 1(a). A thin layer of LiF was vacuum-evaporated on the SnO_2 surface to modify the interface between the electron transport layer (ETL) and the perovskite. The function of the LiF can be found in our recent report [26]. A $CsPbI_{3-x}Br_x$ layer was fabricated by CsI, $HPbI_{3+x}$, and $PbBr_2$, applying the one-step spin-coating method. A black film was obtained after annealing under 170°C. A dopant-free P3HT was spin-coated on perovskite for the HTM. Figure 1(b) shows the band alignment and the charge transport mechanism.

We studied the charge transport properties of P3HT with the perovskite layer using PL. Compared with the perovskite itself and Spiro-OMeTAD depositing, the perovskite film showed a significant PL quench while depositing P3HT on the perovskite surface, indicating that the P3HT has good hole charge extraction for the perovskite layer that is even better than that of Spiro-OMeTAD. The PL emission for the perovskite and perovskite/Spiro-OMeTAD samples was located at 706 nm, while that for the perovskite/P3HT blue shifted to 700 nm, inferring that the P3HT could show a passivation effect while depositing on the perovskite surface [27]. This result could be mainly attributed to the sulfur (S) atoms from P3HT found bonding with the Cs and Pb atoms in the interface (Cs–S: 4.03 Å; Pb–S: 3.36 Å) and suppressing the anti-site defects on the $CsPbI_{3-x}Br_x$ surface [28]. Figure 1(d) shows the corresponding time-resolved PL spectrum. The charge lifetime of the perovskite film with P3HT was much shorter than that with the perovskite and perovskite/Spiro-OMeTAD samples. The lifetimes of $CsPb_{3-x}Br_x$/P3HT, $CsPb_{3-x}Br_x$/Spiro-OMeTAD, and $CsPb_{3-x}Br_x$ were 0.77, 1.50, and 1.93 ns, respectively. The results can further clarify the good carrier extraction at the perovskite/P3HT interface.

Figure 2(a) depicts the representative photocurrent density–voltage (*J–V*) curves of the PSCs based on the P3HT hole-transport layer. The champion cell achieved 15.84% PCE, with the short circuit current density J_{SC} of 18.43 mA/cm^2, the open circuit voltage V_{OC} of 1.12 V, and the fill factor FF of 76.96% measured by reverse scan. While the Spiro-OMeTAD-based device showed a slightly lower performance, the P3HT-based device exhibited a better performance that could be attributed to the perovskite surface passivation of P3HT. Figure 2(b) shows stable reverse and forward scans of 15.28% and 13.13%, respectively. Figure 2(c) depicts the typical

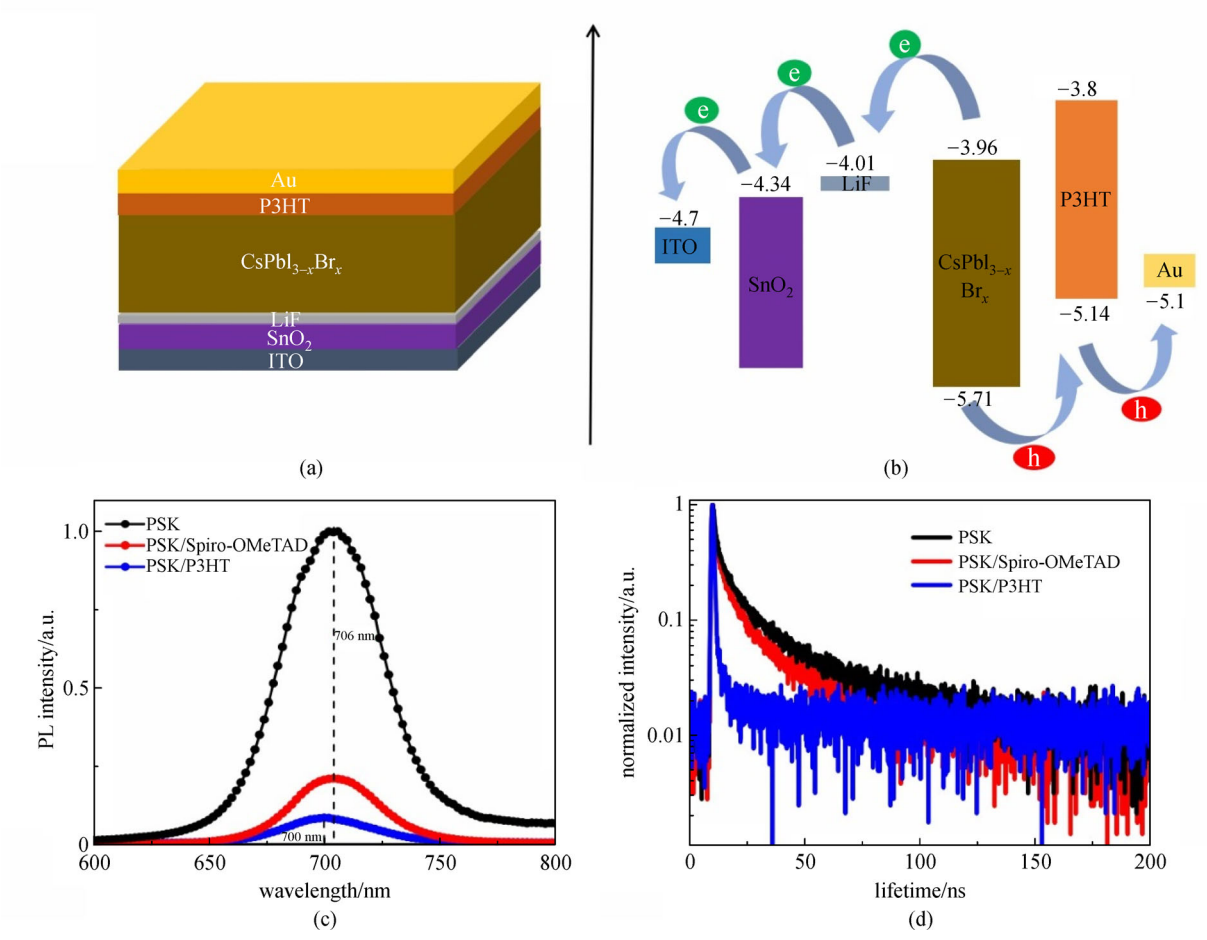

Fig. 1 (a) Device structure of the $CsPbI_{3-x}Br_x$ PSCs based on P3HT. (b) Energy band diagram of $CsPbI_{3-x}Br_x$ PSCs based on P3HT. (c) Steady-state PL spectra of $CsPbI_{3-x}Br_x$ perovskite (PSK), PSK/Spiro-OMeTAD, and PSK/P3HT prepared on glass. (d) Time-resolved PL spectra of $CsPbI_{3-x}Br_x$ PSK, PSK/Spiro-OMeTAD, and PSK/P3HT prepared on glass

external quantum efficiency. The integrated J_{SC} was 17.85 mA/cm^2, which closely matched with the measured J_{SC} from the solar simulator. Figure 2(d) illustrates the performance of the P3HT-based devices with high reproducibility. The average efficiencies of the 40 P3HT- and Spiro-OMeTAD-based devices were approximately 13.5% and 11.3%, respectively.

The ideal factor of the diode is a determinant parameter related to the interfacial defect recombination. The associated formula is nKT/q, where n is the ideal factor, K is the Boltzmann constant, T is the temperature, and q denotes the elementary charge. An n value closer to 1 indicates a lower density of the interfacial traps [29]. We tested the devices' responses under different light intensities to estimate the ideal factor. For comparison, Spiro-OMeTAD was also used as the HTM. Both P3HT- and Spiro-OMeTAD-based devices revealed a linear relationship between the J_{SC} and the light intensity in Fig. 3(a), indicating no significant charge barrier at the interface. As shown in Fig. 3(b), the slope of V_{OC} to the light intensity for the P3HT-based device was $1.58KT/q$, while that for the Spiro-OMeTAD-based device was $1.63KT/q$. This result further confirmed that the P3HT layer can effectively decrease the surface defects at the perovskite/P3HT interface.

We further investigated the thermal stability of the P3HT- and Spiro-OMeTAD-based devices by placing them on a hot plate at 85°C of continuous heating. We then examined the efficiency variation of the devices over time. The efficiency of the Spiro-OMeTAD-based device dropped dramatically within an hour, while that of the device with the P3HT HTM was maintained at 90% of the initial efficiency after 80 h heating (Fig. 4(a)). The photo-stability and the long-term storage stability of the device based on P3HT were also studied. The P3HT-based device can hold 80% of the initial efficiency under a continuous one Sun illumination (100 mW/cm^2) after 300 h (Fig. 4(b)) and drop less than 10% when stored in N_2 glovebox even after 60 d (Fig. 4(c)). These results showed that the P3HT polymer HTM can improve the thermal stability of all-inorganic perovskite devices compared with the Spiro-OMeTAD. Moreover, the P3HT-based all-inorganic

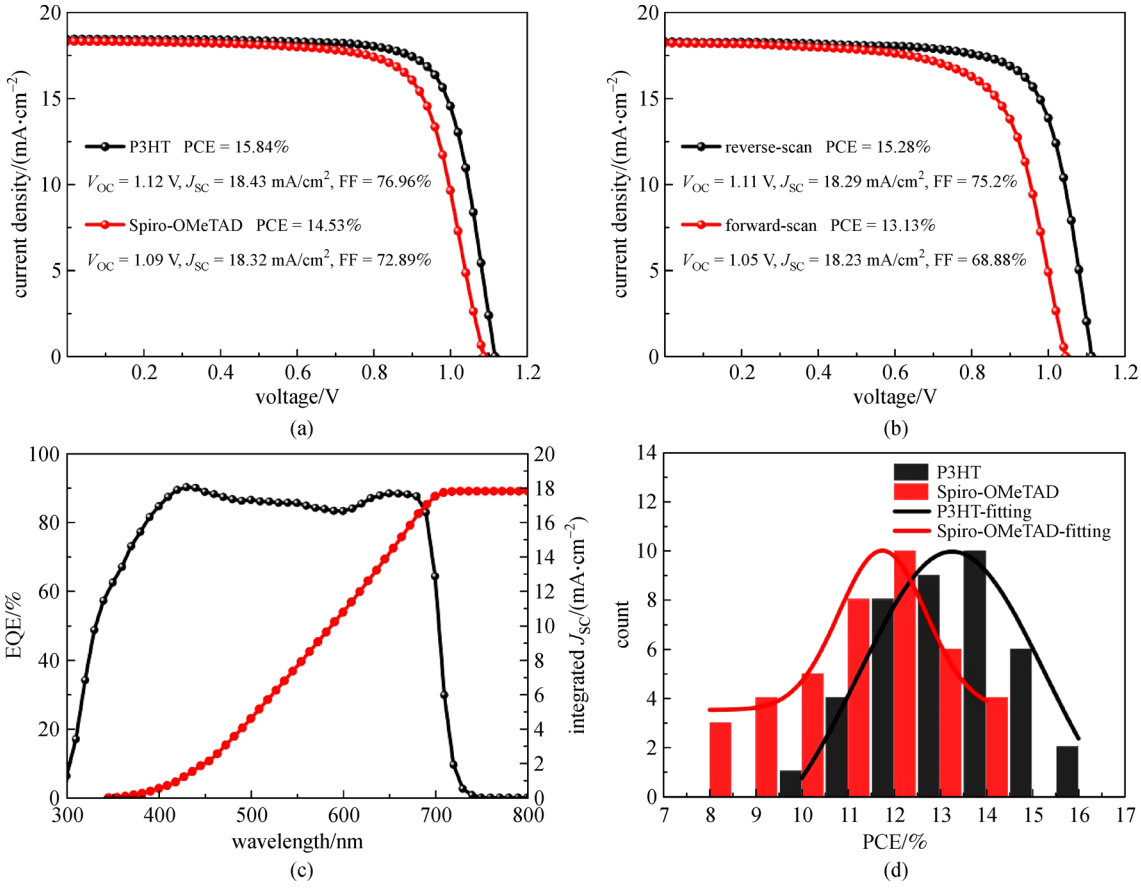

Fig. 2 (a) *J–V* curve of the inorganic $CsPbI_{3-x}Br_x$ PSCs based on different HTMs. (b) Reverse- and forward-scan *J–V* curve from the inorganic $CsPbI_{3-x}Br_x$ PSCs using P3HT as the hole-transport layer. (c) Typical EQE for the devices using P3HT as the hole-transport layer. (d) Efficiency histogram of the inorganic $CsPbI_{3-x}Br_x$ PSCs using different HTMs

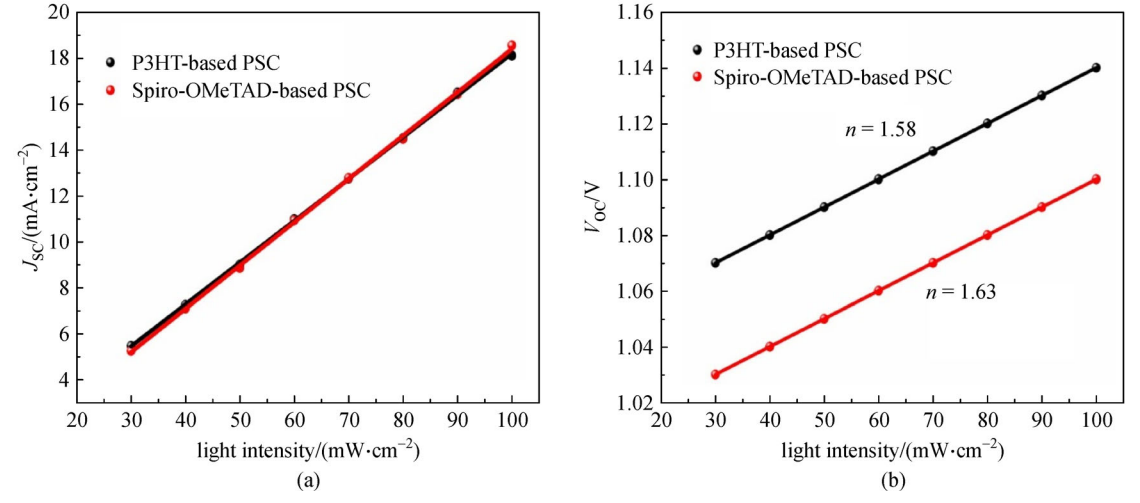

Fig. 3 (a) Relationship between J_{SC} versus light intensity for devices based on different HTMs. (b) V_{OC} versus light intensity for the inorganic $CsPbI_{3-x}Br_x$ PSCs based on different HTMs

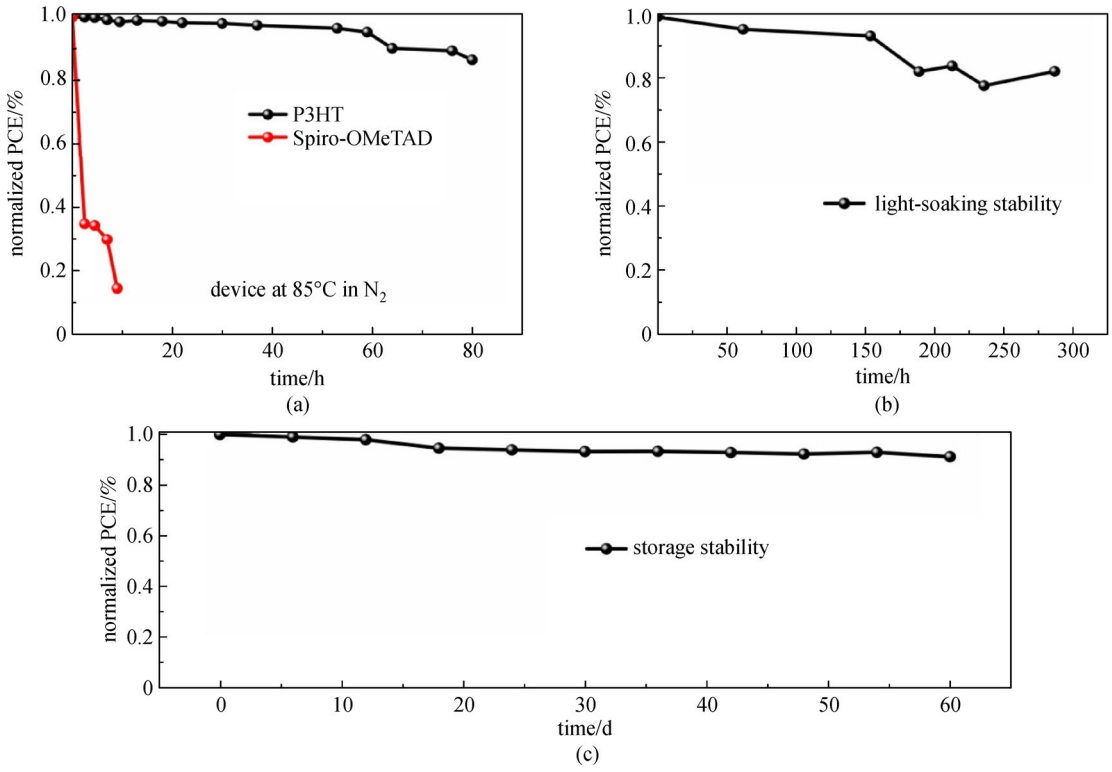

Fig. 4 (a) Thermal stability of $CsPbI_{3-x}Br_x$ PSCs under 85°C in N_2 glove box. (b) Photo-stability of $CsPbI_{3-x}Br_x$ PSCs under continuous white light LED illumination (100 mW/cm^2) in N_2 glove box. (c) Long-term PCE stability of a $CsPbI_{3-x}Br_x$ PSCs without encapsulations stored in a dry glove box and tested once a week

$CsPbI_{3-x}Br_x$ solar cells also showed excellent photo-stability and long-term storage stability. The poor thermal or photo-stability of the Spiro-OMeTAD-based device could be caused by the dopant aggregation or the crystallinity of the Spiro-OMeTAD, which led to poor conductivity or pinholes in the Spiro-OMeTAD and resulted in bad contact or serious recombination. Meanwhile, for the P3HT layer, P3HT was well crystallized, can tolerate a temperature higher than 100°C, and will be very robust under thermal or photo stress [30–32].

4 Conclusions

This study used the dopant-free polymer, P3HT, as the hole-transport layer for inorganic perovskite solar cells. The device showed 15.84% PCE, thereby presenting the best performance among all-inorganic PSCs based on the P3HT HTM. The most important thing herein is that the device can reserve the original efficiency by more than 90% while being heated up to 80 h at 85°C. The efficiency also maintained the initial 85% when irradiated under simulated 1.5 AM sunlight for 300 h.

Acknowledgements This work was supported by the Beijing Municipal Science and Technology Commission (Nos. Z181100004718005 and Z181100005118002).

References

1. Kojima A, Teshima K, Shirai Y, Miyasaka T. Organometal halide perovskites as visible-light sensitizers for photovoltaic cells. Journal of Applied Chemical Science, 2009, 131(17): 6050–6051
2. National Renewable Energy Laboratory (NREL). Best Cell Efficiencies, available at the website of nrel.gov/pv/cell-efficiency (accessed: January 2019)
3. Im J H, Jang I H, Pellet N, Grätzel M, Park N G. Growth of $CH_3NH_3PbI_3$ cuboids with controlled size for high-efficiency perovskite solar cells. Nature Nanotechnology, 2014, 9(11): 927–932
4. Stoumpos C C, Malliakas C D, Kanatzidis M G. Semiconducting tin and lead iodide perovskites with organic cations: phase transitions, high mobilities, and near-infrared photoluminescent properties. Inorganic Chemistry, 2013, 52(15): 9019–9038
5. Dong Q, Fang Y, Shao Y, Mulligan P, Qiu J, Cao L, Huang J. Electron-hole diffusion lengths > 175 μm in solution-grown $CH_3NH_3PbI_3$ single crystals. Science, 2015, 347(6225): 967–970
6. D'Innocenzo V, Grancini G, Alcocer M J, Kandada A R, Stranks S D, Lee M M, Lanzani G, Snaith H J, Petrozza A. Excitons versus free charges in organo-lead tri-halide perovskites. Nature Communications, 2014, 5(4): 3586
7. Zhu H, Miyata K, Fu Y, Wang J, Joshi P P, Niesner D, Williams K W, Jin S, Zhu X Y. Screening in crystalline liquids protects energetic carriers in hybrid perovskites. Science, 2016, 353(6306):

1409–1413
8. Svane K L, Forse A C, Grey C P, Kieslich G, Cheetham A K, Walsh A, Butler K T. How strong is the hydrogen bond in hybrid perovskites? Journal of Physical Chemistry Letters, 2017, 8(24): 6154–6159
9. Chen H, Xiang S, Li W, Liu H, Zhu L, Yang S. Inorganic perovskite solar cells: a rapidly growing field. Solar RRL, 2018, 2(2): 1700188
10. Sim K M, Swarnkar A, Nag A, Chung D S. Phase stabilized α-$CsPbI_3$ perovskite nanocrystals for photodiode applications. Laser & Photonics Reviews, 2018, 12(1): 1700209
11. Mei A, Li X, Liu L, Ku Z, Liu T, Rong Y, Xu M, Hu M, Chen J, Yang Y, Grätzel M, Han H. A hole-conductor-free, fully printable mesoscopic perovskite solar cell with high stability. Science, 2014, 345(6194): 295–298
12. Wang P, Zhang X, Zhou Y, Jiang Q, Ye Q, Chu Z, Li X, Yang X, Yin Z, You J. Solvent-controlled growth of inorganic perovskite films in dry environment for efficient and stable solar cells. Nature Communications, 2018, 9(1): 2225
13. Wang Y, Dar M I, Ono L K, Zhang T, Kan M, Li Y, Zhang L, Wang X, Yang Y, Gao X, Qi Y, Grätzel M, Zhao Y. Thermodynamically stabilized β-$CsPbI_3$–based perovskite solar cells with efficiencies > 18%. Science, 2019, 365(6453): 591–595
14. Wang K, Jin Z, Liang L, Bian H, Bai D, Wang H, Zhang J, Wang Q, Liu S. All-inorganic cesium lead iodide perovskite solar cells with stabilized efficiency beyond 15. Nature Communications, 2018, 9(1): 4544
15. Beal R E, Slotcavage D J, Leijtens T, Bowring A R, Belisle R A, Nguyen W H, Burkhard G F, Hoke E T, McGehee M D. Cesium lead halide perovskites with improved stability for tandem solar cells. Journal of Physical Chemistry Letters, 2016, 7(5): 746–751
16. Wang Y, Zhang T, Kan M, Zhao Y. Bifunctional stabilization of all-inorganic α-$CsPbI_3$ perovskite for 17% efficiency photovoltaics. Journal of the American Chemical Society, 2018, 140(39): 12345–12348
17. Yang F, Hirotani D, Kapil G, Kamarudin M A, Ng C H, Zhang Y, Shen Q, Hayase S. All-inorganic $CsPb_{1-x}Ge_xI_2Br$ perovskite with enhanced phase stability and photovoltaic performance. Angewandte Chemie International Edition, 2018, 130(39): 12927–12931
18. Sanchez S, Christoph N, Grobety B, Phung N, Steiner U, Saliba M, Abate A. Efficient and stable inorganic perovskite solar cells manufactured by pulsed flash infrared annealing. Advanced Energy Materials, 2018, 8(30): 1802060
19. Zeng Q, Zhang X, Feng X, Lu S, Chen Z, Yong X, Redfern S A T, Wei H, Wang H, Shen H, Zhang W, Zheng W, Zhang H, Tse J S, Yang B. Polymer-passivated inorganic cesium lead mixed-halide perovskites for stable and efficient solar cells with high open-circuit voltage over 1.3 V. Advanced Materials, 2018, 30(9): 1705393
20. Bian H, Bai D, Jin Z, Wang K, Liang L, Wang H, Zhang J, Wang Q, Liu S F. Graded bandgap $CsPbI_{2+x}Br_{1-x}$, perovskite solar cells with a stabilized efficiency of 14.4%. Joule, 2018, 2(8): 1500–1510
21. Swarnkar A, Marshall A R, Sanehira E M, Chernomordik B D, Moore D T, Christians J A, Chakrabarti T, Luther J M. Quantum dot-induced phase stabilization of α-$CsPbI_3$ perovskite for high-efficiency photovoltaics. Science, 2016, 354(6308): 92–95
22. Liu J, Wu Y, Qin C, Yang X, Yasuda T, Islam A, Zhang K, Peng W, Chen W, Han L. A dopant-free hole-transporting material for efficient and stable perovskite solar cells. Energy & Environmental Science, 2014, 7(9): 2963–2967
23. Franckevičius M, Mishra A, Kreuzer F, Luo J, Zakeeruddin S M, Gratzel M. A dopant-free spirobi[cyclopenta[2,1-b:3,4-b′]dithiophene] based hole-transport material for efficient perovskite solar cells. Materials Horizons, 2015, 2(6): 613–618
24. Liu Y, Chen Q, Duan H S, Zhou H, Yang Y, Chen H, Luo S, Song T B, Dou L, Hong Z, Yang Y. A dopant-free organic hole transport material for efficient planar heterojunction perovskite solar cells. Journal of Materials Chemistry A, Materials for Energy and Sustainability, 2015, 3(22): 11940–11947
25. Jung E H, Jeon N J, Park E Y, Moon C S, Shin T J, Yang T Y, Noh J H, Seo J. Efficient, stable and scalable perovskite solar cells using poly(3-hexylthiophene). Nature, 2019, 567(7749): 511–515
26. Ye Q, Zhao Y, Mu S, Ma F, Gao F, Chu Z, Yin Z, Gao P, Zhang X, You J. Cesium lead inorganic solar cell with efficiency beyond 18% via reduced charge recombination. Advanced Materials, 2019, 31(49): e1905143
27. Shao Y, Xiao Z, Bi C, Yuan Y, Huang J. Origin and elimination of photocurrent hysteresis by fullerene passivation in $CH_3NH_3PbI_3$ planar heterojunction solar cells. Nature Communications, 2014, 5(1): 5784
28. Zeng Q, Zhang X, Feng X, Lu S, Chen Z, Yong X, Redfern S A T, Wei H, Wang H, Shen H, Zhang W, Zheng W, Zhang H, Tse J S, Yang B. Polymer-passivated inorganic cesium lead mixed-halide perovskites for stable and efficient solar cells with high open-circuit voltage over 1.3 V. Advanced Materials, 2018, 30(9): 1705393
29. Jiang Q, Zhao Y, Zhang X, Yang X, Chen Y, Chu Z, Ye Q, Li X, Yin Z, You J. Surface passivation of perovskite film for efficient solar cells. Nature Photonics, 2019, 13(7): 460–466
30. Leijtens T, Ding I K, Giovenzana T, Bloking J T, McGehee M D, Sellinger A. Hole transport materials with low glass transition temperatures and high solubility for application in solid-state dye-sensitized solar cells. ACS Nano, 2012, 6(2): 1455–1462
31. Abate A, Leijtens T, Pathak S, Teuscher J, Avolio R, Errico M E, Kirkpatrik J, Ball J M, Docampo P, McPherson I, Snaith H J. Lithium salts as “redox active” p-type dopants for organic semiconductors and their impact in solid-state dye-sensitized solar cells. Physical Chemistry Chemical Physics, 2013, 15(7): 2572–2579
32. Tiep N H, Ku Z L, Fan H J. Recent advances in improving the stability of perovskite solar cells. Advanced Energy Materials, 2016, 6(3): 1501420

Shaiqiang Mu received his bachelor degree in Tianshui Normal University, China. He is currently working toward the M.S. degree in Condensed Matter Physics at Zhejiang Normal University, China. He is a joint student in the group of Prof. Shihua Huang and Prof. Jingbi You. His main interests focus on highly efficient all-inorganic perovskite solar cells.

Qiufeng Ye is currently a Ph.D. student under the supervision of Prof. Jingbi You at Key Laboratory of Semiconductor Materials Science, Institute of Semiconductors, Chinese Academy of Sciences, China. His current research focuses on high-efficiency and stable all-inorganic perovskite solar cells.

Xingwang Zhang is a full professor at Institute of Semiconductors, Chinese Academy of Sciences (ISCAS), China. He received his Ph.D. degree in Condensed Matter Physics from Lanzhou University, China in 1999. He did his postdoctoral study at The Chinese University of Hong Kong (CUHK), China from 1999 to 2001. He worked in succession as a visiting scientist and a Humboldt Research Fellow at University of Ulm, Germany from 2001 to 2004. After that he joined Key Laboratory of Semiconductor Materials Science, as a full professor. His current research interests include 2D atomic crystals, photovoltaic materials and devices.

Shihua Huang received his Ph.D. degree in Physics from Fudan University, Shanghai, China in 2004. He is a professor in Department of Physics, Zhejiang Normal University, Jinhua, China. His research interests include the new generation of photovoltaic materials and devices, and the new optoelectronic materials and devices.

Jingbi You is currently a full professor in Institute of Semiconductors, Chinese Academy of Sciences (ISCAS), China. He received his Ph.D. degree in Material Sciences from ISCAS in 2010, and later he did his postdoc at University of California, USA from 2010 to 2015, mainly working in organic tandem solar cells and perovskite solar cells. Since 2015, he joined ISCAS as a full professor. His present research interests are organic/inorganic semiconductor materials and their optoelectronic devices such as solar cells, LEDs, and detectors.